Department of the Interior

U.S. Geological Survey

PETROLOGY, GEOCHEMISTRY AND AGE OF BASANITOIDS DREDGED FROM THE BERING SEA CONTINENTAL MARGIN WEST OF NAVARIN BASIN

by

Alicé S. Davis, Florence L. Wong, Leda-Beth G. Pickthorn, and Michael S. Marlow

Open-File Report 87-407

Menlo Park, California

1987

INTRODUCTION

Quaternary alkalic basalt was recovered in two dredge hauls from the Bering Sea continental margin west of Navarin Basin during the U.S. Geological Cruise L9-82-BS on the R/V S.P. Lee in 1982. The two dredge hauls, D43 and D44, are located at Lat. 58°38.9', Long. 177°13.1' and from 122 m water depth and at Lat. 58°38.9', Long. 177°12.9', and 120 m water depth, respectively (Fig. 1). Other dredges, from greater depths in the same vicinity, recovered calc-alkaline andesite, dacite and tholeiitic basalt of Eocene age. This report presents petrological and geochemical data for the alkalic basalt samples and compares them with Quaternary alkalic basalt from other volcanic centers in the Bering Sea, and with strongly alkalic basalt from oceanic island and continental settings.

METHODS

Samples were studied in thin sections and submitted for bulk chemical analyses to the analytical laboratories of the U.S. Geological Survey. Major element chemistry was determined by wavelength dispersive X-ray fluorescence (XRF) using methods described by Taggart and others (1982). Abundances of Rb, Sr, Zr, Ba, Y, and Nb were determined by energy-dispersive XRF. Precision and accuracy of XRF is 1 to 2% for major elements and 5 to 10% for trace elements. FeO, CO_2, and H_2O were determined by standard wet chemical techniques (Peck, 1964). Abundances of Hf, Ta, Th, Sc, Co, Cr and the rare earth elements (REE) were determined by instrumental neutron activation analysis (INAA) using the method described by Baedecker (1979). Olivine, clinopyroxene and glass compositions were determined with a 9-channel electron microprobe, using 15 kv accelerating voltage and 20 nAmp sample current with a narrowly focused beam (~2 μ) for olivine and clinopyroxene, and 10 nAmp and a larger beam size (~30-50 μ) for glass. Natural and synthetic glasses and minerals were used as standards. Data reduction was performed using a modified version of Bence and Albee's program (1968).

For conventional whole-rock K-Ar measurements, rock was crushed and sieved to retain the 0.5 to 1.0 mm size fraction. The rock powder was acid-leached with HF and HNO_3 to remove clay alteration products. One aliquant was used for the Ar analysis and another was pulverized to a fine powder for duplicate K_2O analyses. K_2O analyses were performed by flame photometry and Ar mass analyses were done with a multiple collector mass spectrometer. Conventional K-Ar dating techniques have been described in detail by Dalrymple and Lanphere (1969).

PETROGRAPHY AND MINERALOGY

Petrography of the samples is summarized in Table 1 and olivine and clinopyroxene analyses are listed in Tables 2 and 3, respectively. Two of the samples (44-8, 44-9) are hyaloclastites composed of fresh, pale-brown sideromelane fragments, with euhedral olivine and clinopyroxene microphenocrysts, disseminated in a yellow to greenish devitrified glass matrix, that contains broken olivine and clinopyroxene crystals. The other samples are highly vesicular (30-55%) flow rock with olivine and clinopyroxene microphenocrysts in a cryptocrystalline or opaque matrix. At high magnification, the opaque tachylite can sometimes be resolved into red-brown glass diffused with specks of equant, opaque minerals. Plagioclase and/or nepheline are not positively identified in any of the thin sections. Similar alkalic lava from the Pribilof Islands, with modal plagioclase but no nepheline have been called basanite, and lava in which both plagioclase and nepheline were absent have been called limburgite (Barth, 1956). Barth reported basanite and limburgite formed from the same flow, depending only on cooling history, with limburgite forming at more rapidly chilled margins and toes. He also observed that the margins of flows were highly vesicular becoming less vesicular toward the interior. The highly vesicular dredge samples probably are rapidly chilled,

scoriaceous margins of basanite flows that were preferentially sampled when the dredge bag was dragged across the surface. Except for the devitrified glass in the hyaloclastites, the dredged samples are fresh and show only traces of clay minerals, calcite and zeolites in fractures and some vesicles.

Olivine is fresh and has no iddingsite alteration rims. Most crystals are very small (<0.5mm), typically euhedral but with slight cuspate margins indicative of resorption. Olivine shows a compositional range from Fo_{81} to Fo_{89} but most are clustered between Fo_{82} and Fo_{84} (Table 2, Fig. 2a). Compositional zoning is absent or minor, showing mostly normal or minor reverse zoning of 1 to 2%, with both occurring in the same sample. Clinopyroxene also shows a limited range in composition with Wo_{45-49}, En_{39-46}, Fs_{8-12} (Table 3, Fig. 2b). Clinopyroxene crystals are brownish-pink, similar in size to olivine, and largely euhedral to subhedral, indicating that they crystallized simultaneously with the olivine. Some broken fragments of clinopyroxene are present but do not differ compositionally from the euhedral crystals. Similar to olivine, some clinopyroxene crystals have hollow cores and irregular margins indicative of resorption. Compositional zoning is slight (2% max.) and may show more magnesian cores with rims somewhat richer in iron or the reverse. Due to the undifferentiated nature of the lava, Ca-Mg-Fe composition is limited (Fig. 2b), however the range in Ti_2O, Al_2O_3, and Cr_2O_3 is considerable, ranging from 1.2 to 3.0%, 2.2 to 6.1%, and 0.01 to 0.92%, respectively.

MAJOR ELEMENT CHEMISTRY

The dredged samples have a narrow compositional range (Table 4). Compositions are relatively primitive with MgO ranging from 9% to 11% for the whole-rock samples. Fresh sideromelane contained within the hyaloclastites has only 5% MgO. Decrease in MgO of about 5% can result from crystal fractionation of approximately 10% olivine and 5% clinopyroxene. The general lack of alteration of the flow samples is indicated by water content of 1% or less, whereas the hyaloclastite samples contain as much as 15% H_2O. Likewise, Fe_2O_3/FeO ratios of less than 0.5 for the flow samples compared to 1.7 for the hyaloclastites is indicative of the degree of oxidation of the latter. Normative compositions of all samples except the hyaloclastites are strongly nepheline-normative (8%-12%). Normative compositions calculated for the whole-rock analyses of the hyaloclastites are hypersthene-normative due to the oxidation and alteration of most of the glass matrix. The fresh sideromelane composition determined by microprobe has more than 11% normative nepheline, calculated with Fe^{3+}=0.25 Fe total. On an alkalies vs. silica plot, all samples, including the hyaloclastites, are clearly alkalic but somewhat less undersaturated in silica than typical basanite from oceanic islands (Fig. 3). These rocks will herein be called basanitoids, following the definition of Macdonald and Katsura (1964) who define basanitoids as alkali olivine basalt containing more than 5% normative nepheline but without modal nepheline. A further division into basanitoid and limburgite based on presence or absence of plagioclase and/or nepheline in the groundmass appears unwarranted because these minerals are occluded in the groundmass due to rapid quenching.

Na, K and Al contents generally increase with decreasing Mg, but the other elements show no well developed trends. Lack of strong element to element correlation is in part due to the limited extent of differentiation. However, even elements that show considerable variation such as Ti and K, show no well-defined linear trends (e.g. Fig. 4). Sulfur content of the glass is about 400 ppm and indicates that these samples are at least partially degassed, and were probably erupted subaerially or into shallow water.

TRACE ELEMENT CHEMISTRY

The basanitoids have a narrow range in trace element composition. Table 5 presents trace element data for the nine whole-rock samples; fresh sideromelane was not abundant enough to separate for trace element analysis. Chondrite-normalized rare earth element (REE) abundances are shown in Figure 5. All of the dredged samples show steep slopes with light REE-enrichment over heavy REE that is typical of alkalic lava, with La/Sm ranging from 3.2 to 4.1 and Ce/Yb from 12 to 19. La abundances range from 126 times chondrite in the hyaloclastite to 193 times chondrite for one of the flow rocks (44-6). Yb abundances ranges from 5.5 to 8.5 times chondrite.

Abundances of compatible elements such as Sc, Co, Cr, which are sensitive to crystal fractionation, are identical, within analytical precision, in all of the flow samples and somewhat lower in the hyaloclastites. In part, this probably reflects fractionation of olivine and clinopyroxene. However, Rb, Sr, Ba which should increase in the melt with fractionation are also lower in the hyaloclastites. Hence, lower concentrations of these mobile elements may be the result of alteration of the glass by seawater. High field strength elements such as Y, Zr and Nb, which are more resistant to alteration, show this effect somewhat less, and ratios of Zr/Nb (4±0.2) and Zr/Hf (43±2) show hardly any variation. Likewise the REE patterns of the hyaloclastite are parallel to those of the flow samples, supporting the contention of Staudigel and Hart (1983) that REE compositions of volcanic glass are not significantly changed by small to moderate amounts of alteration. Abundances of Hf, Ta, and Th are somewhat lower in the hyaloclastites but show no significant change in proportion to each other. All samples plot in a tight cluster in the alkaline within-plate field of the Hf-Ta-Th diagram (Fig. 6, Wood and others, 1980).

K/Rb ratios of about 300 to 500 and high Rb abundance (>50 ppm) (Fig. 7) suggest partitioning of incompatible elements into the melt that is compatible with small amounts of partial melting. Variations in La/Sm (Table 5) and Ce/Yb vs. Ce abundance (Fig. 8) suggest minor variation in percentage of partial melting, although all samples appear to have been generated by very small percentage of melting (< 3%). Kay and Gast (1973) on basis of REE and other trace element studies proposed that chemical differences between alkali basalt, basanite and nephelinite can be explained by having formed by progressively lower extent of partial melting. The solid line on the Ce/Yb vs. Ce plot (Fig. 8) represents the equilibrium batch melting curve of a garnet lherzolite source (55% olivine, 25% orthopyroxene, 15% clinopyroxene, 5% garnet) and a source composition of about 4 times chondrite and a Ce/Yb ratio greater than 2. The Bering Sea basanitoids lie on the extreme end of the steeper curve compatible with melting of a garnet-bearing source, requiring a source more enriched than MORB.

No isotopic data is available for the basanitoids. However, an indication of source homogeneity can be obtained by looking at ratios of trace elements with similar partition coefficients that are not fractionated by partial melting. For example, Ta/Th ratios vary little if percentage of partial melting is large because both have low partition coefficients (near 0.01, Bogault and others, 1979). However, with very small percentage of melting, small differences in partition coefficients become significant, and the Ta/Th ratio can be somewhat fractionated. If the difference between the coefficients is large, as for example for Hf and Ta (0.1 vs. 0.01), a larger variation in the Hf/Ta ratio will result with increased percentage of partial melting (Bogault et al., 1979). A Hf/Ta vs. Ta/Th plot (Fig. 9) indicates a homogeneous source for the Navarin basanitoids, that is distinct from those of St. Paul and St. George.

K-AR AGES

Conventional whole-rock K-Ar ages obtained from the dredged samples range from 0.35 ±0.05 Ma to 1.1 ±0.2 Ma (Table 6). The large errors assigned to these ages result primarily from the imprecision of the age dating method when applied to rocks having a low ratio of radiogenic to atmospheric argon (Dalrymple and Lanphere, 1969). The rocks are very fresh, except for minor

alteration along some fractures and in some vesicles, which should have been removed by the acid treatment. The age data suggests that the dredged samples were erupted during at least two different episodes of volcanism at about 0.4 and 1 Ma.

COMPARISON WITH OTHER ALKALIC LAVA FROM THE BERING SEA

Quaternary basalt of strongly alkalic nature has been reported from the Pribilof Islands and dredged from a submarine ridge (DR1 and DR5) south of the islands (Barth, 1956; Lee-Wong and others, 1979). Basaltic rocks from the Pribilof Islands and ridge show greater variation in composition ranging from tholeiitic and mildly alkalic olivine basalt to basanite and nephelinite. Samples from St. George, the southern island, and samples from the submarine ridge are largely hypersthene-normative to mildly alkalic in composition, although strongly alkalic compositions are also present. St. Paul, located 70 km to the north, erupted only nepheline-normative alkalic lava that closely resembles the basanitoids dredged from the continental margin west of Navarin Basin (Fig. 3). The Pribilof basalts, as a group, also show a limited degree of differentiation; although compositions from St. George and the submarine ridge are more differentiated with some samples approaching hawaiite in composition. Al_2O_3, Na_2O, K_2O, P_2O_5 and TiO_2 increase generally with decreasing MgO but do not show a narrow linear trend as would be expected if simple crystal fractionation were the major process in generating compositional diversity (e.g. Fig. 4). Mineral compositions of samples from St. Paul are similar to those in the basanitoids from west of Navarin Basin, but samples from St. George and the submarine ridge show much greater diversity. Olivine compositions range from Fo_{50} to Fo_{86} (Fig. 2a) and clinopyroxene compositions show a limited iron enrichment trend (Fig. 2b), as might be expected for hypersthene-normative lava. Trace element data (Figs. 6,7,8) indicate that variation in degree of partial melting is the controlling factor in generating the compositional diversity of the Pribilof basalt. The hypersthene-normative and mildly alkalic lava of St.George and the submarine ridge were generated by larger degree of partial melting than the more strongly alkalic lava of St. Paul. However, minor basanite and nephelinite from St.George represent partial melts as small as the most alkalic samples from St. Paul. The basanitoids from the vicinity of Navarin Basin represent even smaller percentage of partial melting than those of St. Paul, if a similar source is assumed (Fig. 8). However, on the Ta/Th vs. Hf/Ta plot (Fig. 9), St. George, St. Paul and the Navarin basanitoids form three distinct clusters suggesting slightly different mantle source compositions for these suites. Furthermore, intra-island heterogeneity is indicated for lava from St. George (Fig. 9). Available isotopic data for alkali olivine basalt from St. George indicates that these samples are isotopically intermediate between MORB and oceanic island basalt (Von Drach and others, 1986). No isotopic data for the hypersthene-normative lava from St. George is available to confirm heterogeneity suggested by trace elements (Fig. 9).

COMPARISON WITH BASANITES FROM OCEANIC ISLANDS

Basaltic rocks that are strongly undersaturated in silica are also found on oceanic islands. Hawaiian and Samoan volcanoes erupt small volumes of strongly alkalic lava during a rejuvenation period that may occur several million years after the main volcanic edifice has been built (Natland, 1975; Clague, 1987). Except for one sample from a seamount which has comparable SiO_2 content (Hawkins and Natland, 1975), basanites and nephelinites from Samoa are more strongly undersaturated than the basanitoids dredged from the vicinity of Navarin Basin (Fig. 3). Samoan basanites appear to be higher in TiO_2 at comparable P_2O_5 (Fig. 4) than either Hawaiian or Bering Sea basanites. However, K and Rb show a trend similar to that of the basanitoids from the vicinty of Navarin Basin. Samoan basanite and nephelinite also were generated by smaller degree of partial melting than the mildly alkalic basalt forming the main edifice (Hawkins and Natland, 1975). Compared to

the Pribilof Islands much greater volumes of mildly alkalic lava were involved in building the main edifices of Samoan Islands. Furthermore, Samoan alkalic lava must have experienced a lengthy period of storage in a magma chamber since abundant highly differentiated trachyte and phonolite are present.

COMPARISON WITH BASANITES FROM A CONTINENTAL SETTING

Strongly alkalic basalt similar to those erupted in the Bering Sea have also been erupted in continental settings, as for example in Antarctica. In a belt nearly 2000 km long, running roughly parallel to the Transantarctic Mts., a volcanic sequence ranges from basanite to phonolite in composition (Goldich and others, 1975; Sun and Hanson, 1975). The basanitoids appear slightly more undersaturated in silica than those from the Bering Sea but less than those from Samoa (Fig. 3). Mineralogically, the Antarctic basanitoids are olivine and clinopyroxene phyric, and show intersertal and intergranular textures, with a groundmass of granular clinopyroxene, opaque minerals, plagioclase ±nepheline indicative of less rapid cooling. Olivine compositions also cluster around Fo_{80} and clinopyroxene is titaniferous augite (Goldich and others, 1975). Element vs. element plots of the Antarctic basanitoids, like the Bering Sea ones, show no strong linear trends for basaltic compositions. However the differentiated sequence from trachybasalt to phonolite shows a strong linear trend indicative of crystal fractionation (Goldich and others, 1975). Diversity within the basanitoids also seems to be primarily the result of different percentages of partial melting. Similar to lava from the Bering Sea, basanitoid and nephelinite represent smaller degrees of partial melting than the mildly alkalic, differentiated basalt sequence (Sun and Hanson, 1975). However a LREE-enriched source is also required, and trace elements and isotopic data clearly indicate chemically and mineralogically heterogeneous mantle sources for the Antarctic samples (Sun and Hanson, 1975).

DISCUSSION AND CONCLUSIONS

The basanitoids from the continental margin west of the Navarin Basin probably erupted from fissures and small vents either subaerially or below seawater at shallow depths. The magma originated at great depth in the upper mantle by a small percentage of partial melting of a garnet lherzolite source, ascended rapidly and was quenched on the seafloor. Limited crystal fractionation of olivine and clinopyroxene probably occurred at intermediate to shallow depths. Small variations in composition are the result of variation in percentage of partial melting of a homogeneous source, although the amount of partial melting was small for all samples (<3%).

Basanitoids of similar composition occur in and near the Pribiloff Islands. They have also been reported from Nunivak and St. Lawrence Islands and from the Seward Peninsula in Alaska (Hoare and others, 1968; Moll-Stalcup, 1987). Detailed petrologic and radiometric age data for this region is sparse; however, Hoare and others (1968) and Moll-Stalcup (1987) suggest that, at least for Nunivak, small volumes of strongly alkalic lava preceded and followed eruption of larger volumes of less alkalic lava. On Nunivak at least five distinct volcanic episodes separated by quiet intervals have occurred in the last 6 m.y. The most recent episode began about 0.3 Ma and so far has erupted only strongly alkalic lava (Hoare and others, 1968). The Pribilof Islands appear to have been built during two pulses of volcanic activity. Activity on St. George began at about 2.2 Ma and ended about 1.6 Ma. After over one million years of quiescence, a second pulse began at 0.4 Ma and produced St. Paul Island, 70 km to the north (Cox and others, 1966). To date only strongly alkalic lava has been erupted. K-Ar data on basaltic rock from the submarine ridge near the Pribilofs suggests an additional volcanic pulse at about 0.8 Ma (Lee-Wong and others, 1979). Basanitoids from west of Navarin Basin also suggest at least two pulses of volcanic activity around 1 and 0.4 Ma. The similar timing of volcanic pulses, associated faulting and alignment of volcanic cones

(west to north-west Hoare and others, 1968) suggests large scale tectonic control.

It is interesting that strongly alkalic lava so similar in composition can be generated in such diverse tectonic settings as oceanic islands, within continental plates and behind an island arc. In each case it appears to involve deep fissures, frequently associated with normal faulting and extension. In Antarctica, the basanitoids erupted in a belt parallel to the Transantarctic Mts., and are probably related to normal faulting. In Samoa, strongly alkalic lava was erupted approximately simultaneously along a chain over 500 km long (Hawkins and Natland, 1975). Hawkins and Natland proposed that a combination of lithospheric flexure and viscous shear melting due to complex interaction of the Pacific plate with the Tonga Trench is responsible for generating the strongly alkalic lava. In the Hawaiian (e.g. Clague, 1987) and Caroline Island chains (Mattey, 1982) the strongly alkalic lava did not erupt simultaneously but shows an age progression similar to that of the main volcanic edifices, which presumably formed as the Pacific plate moved over fixed hot spots. For the Hawaiian chain, Clague and Dalrymple (1987) showed that rejuvenated, strongly alkalic volcanism follows the building of the edifice not by a constant time but by a constant distance. They suggested that the eruption of strongly alkalic lava may be related to change from subsidence to uplift as the volcanoes override the Hawaiian arch (Clague, 1987). A similar process may be operating for the Caroline Islands in relation to the Caroline Ridge. For the widely scattered volcanic centers erupting strongly alkalic lava in the Bering Sea, a more complicated tectonic pattern would be required, but, probably, is somehow related to complex changes in plate motion of the Pacific plate and its interaction with the Aleutian arc.

REFERENCES

Baedecker, P.A., 1979, The INAA program of the U.S. Geological Survey (Reston, Virginia), in Carpenter and others, eds., Computers in activation analysis and γ-ray spectroscopy: Conf.-78042, U.S. Department of Energy, p. 373-385

Barth, T.F.W., 1956, Geology and petrology of the Pribilof Islands, Alaska, in Investigations of Alaskan volcanoes: U.S. Geol. Bull. 1028F, p. 101-160.

Bence, A.E. and Albee, A.E., 1968, Empirical correction factors for the electron microanalysis of silicates and oxides: J. of Geol., v. 76, p. 382-403.

Bogault, H., Joron, J.-L., and Treuil, M., 1979, Alteration, fractional crystallization, partial melting, mantle properties from trace elements in basalts recovered in the North Atlantic, in Talwani and others, eds., Deep sea drilling results in the Atlantic Ocean: Ocean crust. Am. Geophys. Union Maurice Ewing Series 2, p. 352-368.

Clague, D.A., 1987, Hawaiian alkaline volcanism: J. Geol. Soc. London, (in press).

Clague, D.A. and Dalrymple, G.B., 1987, The Hawaiian-Emperor volcanic chain: Part 1. Geologic evolution: U.S. Geological Survey Prof. Paper 1350, p. 5-54.

Cox, A., Hopkins, D.M., and Dalrymple, G.B., 1966, Geomagnetic polarity epochs: Pribilof Islands, Alaska: Geol. Soc. Am. Bull., v.77, p. 883-910.

Dalrymple, G.B. and Lanphere, M.A., 1969, Potassium-Argon Dating: San Francisco, W.H. Freeman Co., 258 p.

Goldich, S.S., Treves, S.B., Suhr, N.H. and Stuckless, J.S., 1975, Geochemistry of the Cenozoic volcanic rocks of Ross Island and vicinity, Antarctica: J. Geol., v.83, p. 415-435.

Haskin, L.A., Haskin M.A., Frey, F.A., and Wildeman, T.R., 1968, Relative and absolute terrestrial abundances of the rare earths, in Ahrens, L.H. ed., Origin and distribution of the elements: New York, Pergamon Press, p. 889-912.

Hawkins, J.W. and Natland, J.H., 1975, Nephelinites and basanites of the Samoan linear volcanic chain: Their possible tectonic significance: Earth Planet. Sci. Lett., v.24, p. 427-439.

Hoare, J.M., Condon, W.H., Cox, A. and Dalrymple, G.B., 1968, Geology, paleomagnetism, and potassium-argon ages of basalts from Nunivak Island, Alaska, in Coats and others, eds., Studies in volcanology: Geol. Soc. Am. Mem., v.116, p. 377-413.

Kay, R.W. and Gast, P.W., 1973, The rare earth content and origin of alkali-rich basalts: J. Geol., v.81, p. 653-682.

Lee-Wong, F., Vallier, T.L., Hopkins, D.M. and Silberman, M.L., 1979, Preliminary report on the petrography and geochemistry of basalts from the Pribilof Islands and vicinity, southern Bering Sea: U.S. Geol. Survey Open-File Report 79-1556, 51p.

Macdonald, G.A. and Katsura, T., 1964, Chemical composition of Hawaiian lavas: J. Petrol., v.6, p. 82-133.

Mattey, D.P., 1982, The minor and trace element geochemistry of volcanic rocks from Truk,

Ponape and Kusaie, eastern Caroline Islands: The evolution of a young hotspot trace across old Pacific Ocean crust: Contrib. Mineral. Petrol., v.80, p. 1-13.

Moll-Stalcup, E., 1987, Cenozoic magmatism in mainland Alaska: in Alaskan Geology: DNAG, Geol. Soc. Am. (in press).

Natland, J.W., 1975, Petrologic studies of linear island chains: Ph.D. dissertation, Univ. Cal., San Diego, 384p.

Peck, L.C., 1964, Systematic analysis of silicates: U.S. Geol. Survey Bull. 1170, 84p.

Staudigel, H. and Hart, S.R., 1983, Alteration of basaltic glass: Mechanisms and significance for the oceanic crust-seawater budget: Geochim Cosmochim. Acta, v.47, p. 337-350.

Sun, S.S. and Hanson, G.N., 1975, Origin of Ross Island basanitoids and limitations upon the heterogeneity of mantle sources for alkali basalts and nephelinites: Contrib. Mineral. Petrol., v.52, p. 77-106.

Taggart, J.E., Lichte, F.E. and Wahlberg, J.S., 1982, Methods of analysis of samples using x-ray fluorescence and induction-coupled plasma spectroscopy, in The 1980 Eruptions of Mount St. Helens, Washington: U.S. Geol. Survey Prof. Pap. 1250, p. 683-687.

Tarney, J., Wood, D.A., Saunders, A.D., Cann, J.R. and Varet, J., 1980, Nature of mantle heterogeneity in the North Atlantic: Evidence from deep sea drilling: Phil. Trans. R. Soc. Lond., v.A 297, p. 179-202.

Von Drach, V., Marsh, B.D. and Wasserburg, G.J., 1986, Nd and Sr isotopes in the Aleutians: multicomponent parenthood of island-arc magmas: Contrib. Mineral. Petrol., v.92, p. 13-34.

Wood, D.A., 1980, The application of a Th-Hf-Ta diagram to problems of tectonomagmatic classification and to establishing the nature of crustal contamination of basaltic lavas of the British Tertiary volcanic province: Earth Planet. Sci. Lett., v.50, p. 11-30.

Table 1: Petrographic Data for Volcanic Rock from the Bering Sea

Sample No.	Texture	Vesicles vol.%	Modal composition (vol.%) Olivine	Clinopyroxene	Groundmass	Remarks
43-2	intergranular	45	15	10	30	cryptocrystalline groundmass, calcite in vesicles
43-9	intergranular	35	15	10	40	cryptocrystalline groundmass clay in vesicles
44-3	intersertal	55	12	8	25	opaque tachylite groundmass
44-6	intergranular	45	15	10	30	cryptocrystalline groundmass
44-7	intergranular	30	12	8	50	opaque tachylite with areas of brown glass and equant opaque minerals
44-8	pyroclastic	10	12	8	70	hyaloclastite of brown sideromelane
44-9	"	"	"	"	"	fragments in devitrified glass matrix
44-10	intergranular	40	6	4	50	tachylite with areas of brown glass and equant opaque minerals
44-11	intergranular	30	16	14	40	cryptocrystalline groundmass
44-12	intergranular	50	10	8	32	cryptocrystalline groundmass
44-13	intergranular to intersertal	50	12	8	30	cryptocrystalline groundmass

* volume % visually estimated

Table 2: Olivine analyses

Sample No.	43-9 1Pr	43-9 1Pc	43-9 m	43-9 m	43-9 2Pr	43-9 2Pc	43-9 m	44-6 m	44-6 1Pr	44-6 1Pc
(wt %)										
SiO_2	39.6	40.0	39.4	39.5	39.7	39.4	39.3	39.9	39.9	39.6
FeO	16.2	14.6	17.4	16.6	15.8	15.8	16.3	15.7	16.3	15.7
MgO	43.5	44.7	42.5	43.2	43.7	43.8	43.3	44.2	43.6	44.2
CaO	0.38	0.23	0.38	0.36	0.31	0.28	0.38	0.28	0.37	0.24
MnO	0.22	0.18	0.24	0.23	0.23	0.21	0.23	0.22	0.24	0.21
NiO	0.18	0.25	0.16	0.17	0.22	0.19	0.19	0.19	0.16	0.24
Total	100.2	100.0	100.1	100.0	100.0	99.6	99.8	100.5	100.6	100.2
				cations based on 4 oxygens						
Si	1.001	1.003	1.001	1.000	1.003	0.989	0.993	1.000	1.004	0.996
Fe	0.342	0.306	0.369	0.352	0.334	0.332	0.345	0.330	0.343	0.330
Mg	1.638	1.672	1.610	1.630	1.643	1.639	1.630	1.654	1.632	1.661
Ca	0.010	0.006	0.010	0.010	0.008	0.007	0.010	0.008	0.010	0.006
Mn	0.005	0.004	0.005	0.005	0.005	0.004	0.005	0.005	0.005	0.004
Ni	0.004	0.005	0.003	0.003	0.004	0.004	0.004	0.004	0.003	0.005
mol Fo%	82.7	84.5	81.4	82.2	83.1	83.2	82.5	83.4	82.6	83.4

Prerim of phenocryst

Pcrcore of phenocryst

mamicrophenocryst

Table 2: olivine analyses continued

Sample No.	44-6 2Pr	44-6 2Pc	44-6 m	44-6 3Pr	44-6 3Pc	44-8 m	44-8 1Pr	44-8 1Pc	44-8 2Pr	44-8 2Pc
(wt %)										
SiO_2	39.5	39.5	39.7	40.3	40.5	39.5	39.4	39.4	39.8	39.5
FeO	16.0	15.1	15.4	10.9	10.9	15.6	16.6	15.7	15.7	15.7
MgO	43.9	44.6	44.1	47.8	47.9	43.5	42.9	43.6	43.6	43.7
CaO	0.38	0.20	0.24	0.08	0.08	0.32	0.42	0.31	0.34	0.30
MnO	0.23	0.18	0.19	0.14	0.14	0.20	0.25	0.19	0.22	0.21
NiO	0.18	0.27	0.24	0.35	0.35	0.20	0.15	0.17	0.18	0.18
Total	100.2	99.8	99.9	99.5	99.8	99.3	99.7	99.4	99.9	99.6
cations based on 4 oxygens										
Si	0.997	0.991	0.990	0.988	0.996	0.985	0.995	0.986	1.004	0.991
Fe	0.337	0.318	0.323	0.222	0.225	0.325	0.351	0.329	0.332	0.329
Mg	1.650	1.668	1.652	1.744	1.756	1.621	1.616	1.628	1.638	1.632
Ca	0.010	0.005	0.006	0.002	0.002	0.009	0.011	0.008	0.009	0.008
Mn	0.005	0.004	0.004	0.003	0.003	0.004	0.005	0.004	0.005	0.005
Ni	0.004	0.005	0.005	0.007	0.007	0.004	0.003	0.003	0.004	0.004
mol Fo%	83.0	83.9	83.7	88.7	88.6	83.3	82.2	83.2	83.2	83.2

Table 2: Olivine analyses continued

Sample No.	44-8 3Pr	44-8 3Pc	44-8 m	44-13 1Pr	44-13 1Pc	44-13 m	44-13 2Pr	44-13 2Pc	44-13 m
(wt %)									
SiO_2	39.4	39.5	39.7	39.2	40.1	39.2	39.4	39.4	39.4
FeO	16.0	15.3	15.6	15.8	15.0	15.6	15.8	16.0	15.1
MgO	43.4	44.2	43.9	43.6	42.9	43.4	43.6	43.7	44.8
CaO	0.36	0.27	0.31	0.34	0.58	0.34	0.36	0.34	0.23
MnO	0.21	0.21	0.22	0.22	0.19	0.22	0.21	0.24	0.20
NiO	0.21	0.21	0.21	0.22	0.21	0.18	0.18	0.12	0.25
Total	99.5	99.6	99.8	99.3	99.0	98.9	99.5	99.7	99.3
				cations based on 4 oxygens					
Si	0.989	0.990	0.998	0.980	0.994	0.976	0.989	0.989	0.983
Fe	0.336	0.320	0.328	0.331	0.312	0.324	0.331	0.336	0.315
Mg	1.623	1.650	1.644	1.625	1.583	1.609	1.629	1.637	1.641
Ca	0.010	0.007	0.008	0.009	0.015	0.009	0.010	0.009	0.006
Mn	0.004	0.004	0.005	0.005	0.004	0.005	0.004	0.005	0.004
Ni	0.004	0.004	0.005	0.004	0.004	0.004	0.004	0.002	0.005
mol Fo%	82.9	83.8	83.4	83.1	83.5	83.2	83.1	83.0	83.9

Table 3: Clinopyroxene analyses

Sample No.	43-9 1Pr	43-9 1Pc	43-9 2Pr	43-9 2Pi	43-9 2Pc	43-9 3Pr	43-9 3Pi	43-9 3Pc	43-9 4Pr	43-9 4Pc	43-9 m	44-6 1Pr
(wt %)												
SiO_2	49.6	47.5	49.2	49.3	49.1	49.1	47.1	49.4	51.1	50.8	51.3	47.6
TiO_2	1.60	2.69	1.64	2.07	2.01	1.87	2.85	2.01	1.25	1.60	1.38	2.64
Al_2O_3	4.11	5.70	4.16	3.83	3.95	4.47	5.83	3.57	2.45	3.15	2.59	5.65
FeO	5.79	6.76	5.75	7.01	7.16	5.89	7.07	7.13	5.47	6.46	5.89	6.45
Cr_2O_3	0.62	0.28	0.88	0.01	0.01	0.88	0.26	0.09	0.50	0.15	0.63	0.24
MnO	0.06	0.10	0.07	0.12	0.11	0.09	0.08	0.11	0.09	0.09	0.08	0.09
MgO	15.0	13.8	15.0	14.6	14.4	14.6	13.4	14.4	16.0	15.1	15.8	13.4
CaO	22.6	22.3	22.4	22.1	22.3	22.5	22.5	22.3	22.3	22.4	22.2	22.9
Na_2O	0.46	0.51	0.47	0.46	0.53	0.49	0.59	0.46	0.38	0.44	0.38	0.50
Total	99.7	99.6	99.5	99.5	99.6	99.8	99.7	99.5	99.6	100.1	100.3	99.5
Cations based on 6 oxygens												
Si	1.832	1.765	1.815	1.822	1.821	1.818	1.756	1.829	1.877	1.880	1.890	1.766
Ti	0.044	0.075	0.045	0.058	0.056	0.052	0.080	0.056	0.034	0.045	0.038	0.074
Al	0.179	0.249	0.181	0.167	0.173	0.195	0.256	0.155	0.106	0.137	0.113	0.247
Fe	0.179	0.210	0.177	0.217	0.222	0.182	0.221	0.221	0.168	0.200	0.182	0.200
Cr	0.018	0.008	0.026	0.000	0.000	0.026	0.008	0.003	0.014	0.004	0.018	0.007
Mn	0.002	0.003	0.002	0.004	0.003	0.003	0.002	0.004	0.003	0.003	0.002	0.003
Mg	0.825	0.762	0.822	0.806	0.798	0.806	0.746	0.795	0.876	0.833	0.870	0.741
Ca	0.893	0.886	0.883	0.877	0.888	0.891	0.900	0.882	0.877	0.888	0.879	0.912
Na	0.033	0.037	0.034	0.033	0.038	0.035	0.043	0.033	0.027	0.032	0.027	0.036
(mol %)												
Wo	47.1	47.7	46.9	46.2	46.5	47.4	48.2	46.5	45.7	46.2	45.5	49.2
En	43.5	41.0	43.7	42.4	41.8	42.9	40.0	41.9	45.6	43.4	45.1	40.0
Fs	9.4	11.3	9.4	11.4	11.6	9.7	11.8	11.6	8.7	10.4	9.4	10.8

Pr=rim of larger phenocryst

Pc=core of larger phenocryst

Pi=intermediate between rim and core

m=microphenocryst

Table 3: Clinopyroxene analyses continued

Sample No.	44-6 1Pc	44-6 2Pr	44-6 2Pi	44-6 2Pc	44-6 3Pr	44-6 3Pi	44-6 3Pc	44-6 4m	44-6 5m	44-6 6Pc	44-6 6Pr	44-6 6Pi
(wt %)												
SiO_2	51.5	47.0	48.1	51.6	49.7	49.4	50.8	50.3	50.5	47.6	51.3	49.5
TiO_2	1.26	2.68	2.33	1.22	2.06	2.08	1.63	1.80	1.83	2.55	1.19	1.71
Al_2O_3	3.04	5.83	5.49	3.10	3.61	4.01	3.03	3.54	3.44	5.14	2.66	4.81
FeO	4.95	6.96	6.38	5.07	6.40	6.74	5.43	5.88	5.97	6.81	5.04	5.44
Cr_2O_3	0.67	0.22	0.31	0.63	0.11	0.07	0.41	0.17	0.14	0.36	0.63	0.84
MnO	0.07	0.06	0.07	0.08	0.09	0.10	0.07	0.08	0.08	0.07	0.05	0.07
MgO	15.4	13.4	13.7	15.6	14.7	14.3	15.4	14.8	14.7	13.5	15.6	14.1
CaO	22.9	22.7	22.9	23.0	23.0	23.0	22.8	23.0	23.0	22.9	22.7	22.4
Na_2O	0.49	0.57	0.46	0.50	0.41	0.45	0.45	0.41	0.39	0.52	0.47	0.62
Total	100.2	99.4	99.7	100.7	100.1	100.1	99.9	99.9	100.1	99.5	99.6	99.5
Cations based on 6 oxygens												
Si	1.893	1.744	1.785	1.889	1.847	1.839	1.875	1.861	1.871	1.769	1.880	1.818
Ti	0.035	0.075	0.065	0.033	0.058	0.058	0.045	0.050	0.051	0.071	0.033	0.047
Al	0.132	0.257	0.240	0.134	0.158	0.176	0.132	0.155	0.150	0.225	0.115	0.208
Fe	0.152	0.216	0.198	0.155	0.199	0.210	0.168	0.182	0.185	0.212	0.155	0.167
Cr	0.019	0.006	0.009	0.018	0.003	0.002	0.012	0.005	0.004	0.010	0.018	0.024
Mn	0.002	0.002	0.002	0.002	0.003	0.003	0.002	0.002	0.003	0.002	0.002	0.002
Mg	0.844	0.741	0.755	0.850	0.816	0.794	0.847	0.819	0.811	0.750	0.854	0.770
Ca	0.901	0.901	0.912	0.902	0.917	0.916	0.901	0.911	0.913	0.910	0.891	0.882
Na	0.035	0.041	0.033	0.036	0.030	0.032	0.032	0.030	0.028	0.037	0.033	0.044
(mol %)												
Wo	47.5	48.5	48.9	47.3	47.5	47.7	47.0	47.6	47.8	48.6	46.9	48.5
En	44.5	39.9	40.5	44.6	42.2	41.4	44.2	42.8	42.5	40.1	44.9	42.3
Fs	8.0	11.6	10.6	8.1	10.3	10.9	8.8	9.5	9.7	11.3	8.2	9.2

Table 3: Clinopyroxene analyses continued

Sample No.	44-6 7Pr	44-6 7Pc	44-6 8m	44-6 9m	44-6 10Pr	44-6 10Pc	44-6 11m	44-6 12m	44-6 13Pr	44-6 13Pc	44-8 1Pr	44-8 1Pc
(wt %)												
SiO_2	50.4	50.4	50.4	47.9	49.7	47.0	50.9	50.3	50.3	50.3	51.0	46.9
TiO_2	1.75	1.60	1.66	2.48	2.13	2.75	1.61	1.69	1.84	1.66	1.43	3.00
Al_2O_3	2.87	2.70	2.76	4.83	3.21	5.27	2.58	2.84	2.84	2.78	2.88	6.11
FeO	5.89	5.57	6.13	6.24	6.86	6.51	5.59	5.87	6.26	5.77	5.85	7.21
Cr_2O_3	0.23	0.34	0.30	0.61	0.13	0.39	0.27	0.22	0.15	0.21	0.35	0.27
MnO	0.06	0.08	0.08	0.06	0.09	0.08	0.06	0.09	0.11	0.07	0.09	0.09
MgO	14.9	15.3	15.1	13.8	14.6	13.3	15.1	15.0	14.8	14.9	15.5	13.2
CaO	23.1	22.9	22.8	22.8	22.7	22.8	23.1	23.1	23.1	23.2	22.6	22.5
Na_2O	0.43	0.36	0.40	0.51	0.37	0.55	0.41	0.38	0.43	0.39	0.41	0.54
Total	99.6	99.3	99.7	99.3	99.8	98.7	99.7	99.5	99.8	99.3	100.1	99.7
Cations based on 6 oxygens												
Si	1.859	1.849	1.864	1.771	1.847	1.728	1.878	1.854	1.866	1.847	1.885	1.749
Ti	0.049	0.044	0.046	0.069	0.060	0.076	0.045	0.047	0.051	0.046	0.040	0.084
Al	0.125	0.117	0.120	0.210	0.140	0.228	0.112	0.123	0.124	0.120	0.126	0.269
Fe	0.182	0.171	0.190	0.193	0.213	0.200	0.172	0.181	0.194	0.177	0.181	0.225
Cr	0.007	0.010	0.009	0.018	0.004	0.011	0.008	0.006	0.004	0.006	0.010	0.008
Mn	0.002	0.002	0.002	0.002	0.003	0.002	0.002	0.003	0.003	0.002	0.003	0.003
Mg	0.819	0.837	0.830	0.760	0.806	0.727	0.832	0.823	0.820	0.817	0.853	0.731
Ca	0.915	0.901	0.904	0.904	0.904	0.898	0.913	0.912	0.916	0.911	0.895	0.898
Na	0.031	0.026	0.029	0.037	0.027	0.039	0.029	0.027	0.031	0.028	0.030	0.039
(mol. %)												
Wo	47.8	47.2	44.7	48.7	47.0	49.2	47.6	47.6	47.5	47.8	46.4	48.4
En	42.7	43.8	45.9	40.9	41.9	39.8	43.4	43.0	42.5	42.9	44.2	39.4
Fs	9.5	9.0	9.4	10.4	11.1	11.0	9.0	9.4	10.1	9.3	9.4	12.1

Table 3: Clinopyroxene analyses continued

Sample No.	44-8 2Pr	44-8 2Pc	44-8 3Pr	44-8 3Pc	44-8 4Pr	44-8 4Pc	44-8 5Pr	44-8 5Pc	44-8 6Pr	44-8 6Pc	44-13 1Pr	44-13 1Pc
(wt %)												
SiO_2	49.2	48.5	50.8	49.4	49.0	51.0	45.9	46.6	49.2	50.8	50.9	51.5
TiO_2	1.81	2.25	1.74	2.01	2.07	1.63	3.24	2.73	1.74	1.57	1.73	1.32
Al_2O_3	4.44	4.51	2.85	3.50	4.40	2.77	6.54	5.74	4.37	2.80	2.69	2.48
FeO	6.02	6.12	6.48	6.96	5.89	6.21	7.55	7.64	5.89	6.35	6.32	5.66
Cr_2O_3	0.82	0.80	0.10	0.04	0.92	0.34	0.17	0.13	0.87	0.34	0.28	0.52
MnO	0.07	0.08	0.09	0.10	0.08	0.10	0.08	0.07	0.07	0.12	0.12	0.07
MgO	14.6	14.2	15.0	14.4	14.5	15.5	12.1	13.1	14.5	15.6	15.4	15.7
CaO	22.6	22.7	22.6	22.7	22.7	22.2	22.5	22.6	22.6	22.0	22.4	22.4
Na_2O	0.48	0.48	0.39	0.39	0.45	0.34	0.57	0.55	0.48	0.35	0.33	0.37
Total	100.0	99.7	100.1	99.5	100.0	100.0	99.4	99.2	99.7	100.0	100.0	100.0
Cations based on 6 oxygens												
Si	1.829	1.801	1.882	1.829	1.823	1.886	1.711	1.733	1.821	1.881	1.884	1.900
Ti	0.051	0.063	0.048	0.056	0.058	0.045	0.091	0.076	0.048	0.004	0.048	0.037
Al	0.194	0.197	0.125	0.153	0.193	0.121	0.287	0.251	0.191	0.122	0.117	0.108
Fe	0.187	0.190	0.201	0.215	0.183	0.192	0.235	0.237	0.182	0.196	0.196	0.175
Cr	0.024	0.023	0.003	0.001	0.027	0.010	0.005	0.004	0.025	0.010	0.008	0.015
Mn	0.002	0.003	0.003	0.003	0.003	0.003	0.002	0.002	0.002	0.004	0.004	0.002
Mg	0.806	0.785	0.831	0.793	0.802	0.852	0.718	0.724	0.801	0.859	0.848	0.865
Ca	0.899	0.903	0.898	0.898	0.902	0.878	0.898	0.900	0.896	0.874	0.887	0.885
Na	0.034	0.034	0.028	0.028	0.032	0.025	0.041	0.040	0.035	0.025	0.024	0.026
(mol. %)												
Wo	47.5	48.1	46.5	47.1	47.8	45.7	48.5	48.4	47.7	45.3	45.9	46.0
En	42.6	41.8	43.1	41.6	42.5	44.3	38.8	38.9	42.6	44.5	43.9	44.9
Fs	9.9	10.1	10.4	11.3	9.7	10.0	12.7	12.7	9.7	10.2	10.2	9.1

Table 3: Clinopyroxene analyses continued

Sample No.	44-13 2m	44-13 3Pr	44-13 3Pc	44-13 4m	44-13 5Pr	44-13 5Pc	44-13 6m	44-13 7Pr	44-13 7Pc	44-13 8m	44-13 9Pr	44-13 9Pc
SiO_2	47.9	48.6	50.8	47.9	49.3	51.8	46.3	49.3	50.3	49.6	50.3	51.3
TiO_2	2.48	2.20	1.48	2.65	2.13	1.16	3.26	1.99	1.52	1.94	2.03	1.54
Al_2O_3	4.92	4.26	2.61	4.86	4.24	2.22	5.69	4.04	3.55	3.97	2.80	2.54
FeO	6.39	6.07	6.10	6.59	6.14	5.10	7.12	6.03	5.46	5.89	6.88	5.91
Cr_2O_3	0.78	0.84	0.47	0.56	0.71	0.64	0.52	0.81	0.90	0.54	0.10	0.32
MnO	0.06	0.08	0.09	0.07	0.05	0.09	0.07	0.07	0.08	0.06	0.09	0.08
MgO	13.9	14.4	15.5	13.7	14.2	16.0	13.1	14.5	15.0	14.7	14.8	15.5
CaO	22.5	22.8	22.1	22.6	22.9	22.7	22.4	22.7	22.6	22.7	22.5	22.8
Na_2O	0.54	0.50	0.41	0.49	0.47	0.42	0.48	0.46	0.45	0.48	0.34	0.35
Total	99.4	99.7	99.5	99.4	100.1	100.1	99.0	100.0	99.9	99.7	99.8	100.3
Cations based on 6 oxygens												
Si	1.773	1.807	1.867	1.773	1.832	1.907	1.714	1.834	1.860	1.833	1.865	1.894
Ti	0.069	0.061	0.041	0.074	0.059	0.032	0.091	0.056	0.042	0.054	0.057	0.043
Al	0.215	0.186	0.113	0.212	0.186	0.096	0.248	0.177	0.155	0.173	0.122	0.111
Fe	0.198	0.189	0.188	0.204	0.191	0.157	0.220	0.188	0.169	0.182	0.213	0.182
Cr	0.023	0.025	0.014	0.017	0.021	0.019	0.015	0.024	0.026	0.016	0.003	0.009
Mn	0.002	0.003	0.003	0.002	0.002	0.003	0.002	0.002	0.002	0.002	0.003	0.003
Mg	0.765	0.796	0.849	0.758	0.786	0.877	0.723	0.806	0.828	0.808	0.815	0.850
Ca	0.893	0.906	0.872	0.897	0.912	0.897	0.888	0.905	0.897	0.898	0.895	0.900
Na	0.039	0.036	0.029	0.035	0.034	0.030	0.034	0.033	0.032	0.034	0.024	0.025
(mol. %)												
Wo	48.1	47.9	45.7	48.3	48.3	46.5	48.5	47.7	47.4	47.6	46.5	46.6
En	41.2	42.1	44.5	40.8	41.6	45.4	39.5	42.4	43.7	42.8	42.4	44.0
Fs	10.7	10.0	9.8	11.0	10.1	8.1	12.0	9.9	8.9	9.6	11.1	9.4

Table 4: Major element analyses and normative mineral composition of basanitoids dredged from the continental margin in the Bering Sea

Sample No.	44-3	44-6	44-7	44-8	44-8 Glass	44-9	44-9 Glass	44-10	44-11	44-12	44-13
(wt %)											
SiO_2	41.5	43.2	44.8	38.6	46.3	42.4	46.4	45.3	44.6	43.9	45.4
Al_2O_3	10.6	11.2	11.4	9.61	13.0	9.59	13.3	11.6	11.3	11.5	11.6
Fe_2O_3	4.84	3.64	3.63	7.68	--	8.17	--	3.01	3.59	4.46	3.69
FeO	7.34	8.87	8.97	4.34	11.5*	5.16	11.6*	9.08	9.10	8.04	8.74
MgO	10.6	10.5	9.24	10.2	5.13	8.96	5.03	9.58	9.40	9.47	8.91
CaO	11.0	10.9	10.5	5.03	10.6	5.67	10.4	10.4	10.3	10.3	10.1
Na_2O	3.09	3.54	3.45	2.59	4.22	2.94	4.33	3.42	3.51	3.52	3.41
K_2O	1.91	2.30	2.23	1.59	2.47	1.84	2.44	2.06	2.20	2.17	2.16
TiO_2	3.27	3.41	3.27	2.70	3.73	2.66	3.66	3.21	3.24	3.24	3.16
P_2O_5	1.24	0.86	0.84	0.78	0.79	0.80	0.87	0.90	0.82	0.88	0.92
MnO	0.16	0.16	0.15	0.13	0.16	0.11	0.16	0.15	0.15	0.15	0.15
H_2O^+	0.93	0.29	0.56	4.58	--	3.91	--	0.57	0.57	0.55	0.73
H_2O^-	1.02	0.19	0.56	11.27	--	7.78	--	0.34	0.60	0.59	0.56
CO_2	0.21	0.21	0.12	0.31	--	0.19	--	0.08	0.08	0.12	0.10
S (ppm)	--	--	--	--	450	--	350	--	--	--	
Total	97.7	99.1	99.7	99.8	98.0	100.2	98.2	99.7	99.3	98.8	99.5
CIPW Normative Mineral Composition -- Volatile-free											
Or	11.8	13.8	13.4	11.3	14.8	12.3	14.6	12.3	13.2	13.1	13.0
Ab	7.38	2.99	10.5	26.3	14.6	28.2	9.77	12.5	10.3	10.4	14.9
An	9.85	7.99	9.17	11.9	9.39	8.54	11.4	9.12	10.8	10.9	7.9
Ne	11.4	14.8	10.4	--	11.8	--	11.6	9.12	10.8	10.9	7.87
Wo	16.2	17.2	15.9	4.99	16.2	7.27	15.3	10.0	10.7	11.2	9.82
En	12.4	12.1	10.8	13.7	9.32	19.0	9.00	10.0	10.7	11.2	9.82
Fs	2.06	3.67	3.92	--	6.16	--	5.59	3.86	3.95	2.85	3.57
Fo	10.7	10.1	8.82	11.8	2.57	4.43	2.58	9.90	9.24	9.08	8.95
Fa	1.95	3.40	3.53	--	1.87	--	1.76	4.19	3.77	2.55	3.58
Mt	7.34	5.35	5.34	7.91	4.27	10.5	4.83	4.42	5.30	6.62	5.45
Hm	--	--	--	3.77	--	2.00	--	--	--	--	--
Il	6.50	6.57	6.31	6.16	7.20	5.72	7.04	6.18	6.27	6.30	6.11
Ap	3.07	2.07	2.02	2.22	1.90	2.15	2.09	2.16	1.98	2.14	2.22

*total iron as FeO, Fe^{3+}=0.25 Fe total for norm calculations

XRF analysis by A. Bartel and K. Stewart, proj. leader J. Taggart

FeO, CO_2, H_2O analysis by L. Espos, proj. leader W. Updegrove

Table 5: Trace element analyses of basanitoids dredged from the continental margin in the Bering Sea

Sample No.	44-3	44-6	44-7	44-8	44-9	44-10	44-11	44-12	44-13
*									
Rb	46	60	56	23	35	56	51	59	67
Sr	916	874	831	451	513	822	796	838	789
Y	17	21	20	17	17	19	18	20	24
Zr	246	258	233	196	192	237	233	241	233
Nb	58	65	61	51	46	59	57	59	63
Ba	1012	793	689	542	477	696	644	702	643
**									
Hf	5.7	5.8	5.5	4.6	4.4	5.4	5.4	5.8	5.3
Ta	4.2	4.4	4.2	3.4	3.3	3.9	4.0	4.3	3.9
Th	7.6	8.4	7.1	5.6	5.3	6.6	6.9	7.3	6.3
La	56.9	63.6	55.1	44.3	41.6	52.0	53.3	56.6	52.0
Ce	104	110	99.1	81.0	75.3	93.5	95.9	103	92.1
Sm	7.7	9.9	9.4	6.6	6.6	9.1	9.3	9.5	8.1
Eu	2.8	2.8	2.7	2.1	2.1	2.6	2.6	2.7	2.5
Tb	0.93	0.88	0.94	0.71	0.65	0.90	0.94	0.99	0.84
Yb	1.3	1.3	1.6	1.1	1.4	1.4	1.6	1.7	1.5
Lu	0.19	0.20	0.20	0.16	0.16	0.19	0.18	0.20	0.21
Sc	19.5	18.6	18.9	15.4	15.3	18.9	18.0	18.9	17.9
Co	56.1	56.4	53.7	44.0	44.8	53.6	52.4	55.3	51.8
Cr	213	223	224	179	175	216	213	228	201
K/Rb	345	319	331	574	436	305	326	305	268
K/Ba	15.4	24.1	26.9	24.3	32.0	24.6	28.4	25.7	27.9
Zr/Nb	4.2	4.0	3.8	3.8	4.2	4.0	4.1	4.1	3.7
Zr/Hf	43.2	44.5	42.4	42.6	43.6	43.9	43.2	41.6	44.0
$(Ce/Yb)_N$	18.2	19.2	14.1	16.8	12.2	15.2	13.6	13.8	14.0
$(La/Sm)_N$	4.1	3.5	3.2	3.7	3.5	3.1	3.1	3.3	3.5
Hf/Ta	1.32	1.32	1.31	1.35	1.36	1.38	1.35	1.35	1.36
Ta/Th	0.55	0.52	0.59	0.61	0.62	0.59	0.58	0.59	0.62

*XRF analysis, analysts R. Johnson and K. Dennen, proj. leader J. Lindsay

** INAA analysis, analyst J.S. Mee, proj. leader C.A. Palmer

Table 6: Whole rock K/Ar ages of basaltic rock dredged from the Bering Sea

Sample No.	K_2O (wt.%)	$^{40}Ar_{rad}$ ($x10^{-13}$ mol/gm)	$^{40}Ar_{rad}/^{40}Ar_{total}$	Calculated age (m.y.)	Assigned age (m.y.)
43-2	1.424	6.813	0.034	0.33	0.42±0.15
	1.416	10.025	0.046	0.50	
44-3	0.605	5.380	0.054	0.6	0.6±0.2
	0.608				
44-7	1.542	8.493	0.037	0.38	0.35 ±0.05
	1.544	7.394	0.030	0.33	
44-12	0.757	12.57	0.053	1.1	1.1±0.2
	0.758				

Age constants: $\lambda_{e+e'} = 0.581x10^{-10}$ yr^{-1}, $\lambda_B = 4.962x10^{-10}yr^{-1}$, $^{40}K/K = 1.167x10^{-1}$ atom percent

FIGURE CAPTIONS

Figure 1. Map of the Bering Sea continental shelf and slope showing dredge locations of the basanitoids from Navarin Basin and of dredge hauls near the Pribilof Islands.

Figure 2. (a) Histogram of olivine forsterite content (Fo % molar) in basanitoids from west of Navarin Basin (stippled) compared with Fo content of olivine in alkalic basalt from the Pribilof Islands (striped). Samples from west of Navarin Basin show a narrow range with Fo clustered around 82 to 84, whereas the Pribilof basalts range from Fo_{50} to Fo_{86}. (b) Ternary Ca-Mg-Fe diagram for clinopyroxene in Navarin basanitoids shows a restricted range. Compositions of clinopyroxene from St. Paul are similar but those from St. George and the submarine ridge show greater diversity with a limited iron enrichment trend.

Figure 3. Alkalies vs. silica plot for lava dredged from west of Navarin basin. Pribilof basalts shown for comparison include some less alkalic compositions from St. George and from the submarine ridge (DR1 and DR5). St. Paul lava is comparably undersaturated in silica. Except for one sample from a Samoan seamount, compositions of strongly alkalic lava from Samoa and from Ross Island, Antarctica are more strongly undersaturated than those from the Bering Sea. Averaged composition of Hawaiian basanites is shown for comparison. Data for Samoa from Hawkins and Natland (1975) and for Antarctica from Goldich and others, (1975). Pribilof data includes compositions of Barth (1956) and Lee-Wong and others, (1979). Field of alkalic vs. tholeiitic composition after Macdonald and Katsura (1964).

Figure 4. TiO_2 vs. P_2O_5 plot of Navarin basanitoids and Pribilof Islands show increase in TiO_2 and P_2O_5 with alkalinity and smaller amounts of partial melting, but the large scatter suggests that a Ti-bearing phase may be retained in the residuum. Samoan basanites are higher in TiO_2 than the other suites.

Figure 5. Chondrite-normalized rare earth element patterns for basanitoids from the western continental margin show a narrow range of parallel patterns with steep slopes typical of strongly alkalic lava. Field of Pribilof Island basalts shows a greater range in composition and includes some positive Eu anomalies suggestive of plagioclase accumulation. Data normalized to nine chondrites of Haskins and others, (1968).

Figure 6. On a Hf-Th-Ta plot basanitoids from west of Navarin Basin form a tight cluster in the alkaline within-plate field (Wood and others, 1980). Most of the Pribilof Island basalts fall into the same field but some of the hypersthene-normative samples straddle the boundary with oceanic island and E-type MORB.

Figure 7. K_2O vs. Rb plot shows the basanitoids from the western continental margin on the same general trend as Samoan (S) and Antarctic (A) basanites, however large scatter or multiple trends are observed for the Pribilof Islands. Data for Samoa from Hawkins and Natland (1975) for Ross Island from Goldich et al. (1975) and Sun and Hanson (1975). K/Rb ratios of approximately 350, 450 and 750 are shown for reference.

Figure 8. Plot of chondrite-normalized Ce/Yb ratios vs. normalized Ce abundance for alkalic lava from the Bering Sea indicates a small percentage of partial melting for the basanitoids from west of Navarin basin and progressively increasing degree of melting for lava from St. Paul and St. George. The solid curved line indicates a batch melting curve for

garnet lherzolite. Compositions at 30% to 1% partial melting are indicated. Note that a source more enriched than MORB, with heavy REE about 3 to 4 times chondrite and $(Ce/Yb)_N$ >2, would be required to generate these compositions. Due to the nature of the log-log plot the curve can be moved relative to its axes. Modified from Tarney and others, (1980).

Figure 9. Ta/Th vs. Hf/Ta plot for Bering Sea alkalic basalt indicates that the basanitoids from west of Navarin basin were generated from a homogeneous mantle source that is distinct from those of St. Paul and St. George. Strongly alkalic lava of St. George apparently was derived from a different source than the hypersthene-normative samples, but from one similar to that of St. Paul. Variation within each field is probably the result of different degrees of partial melting. Symbols as in Fig. 2.

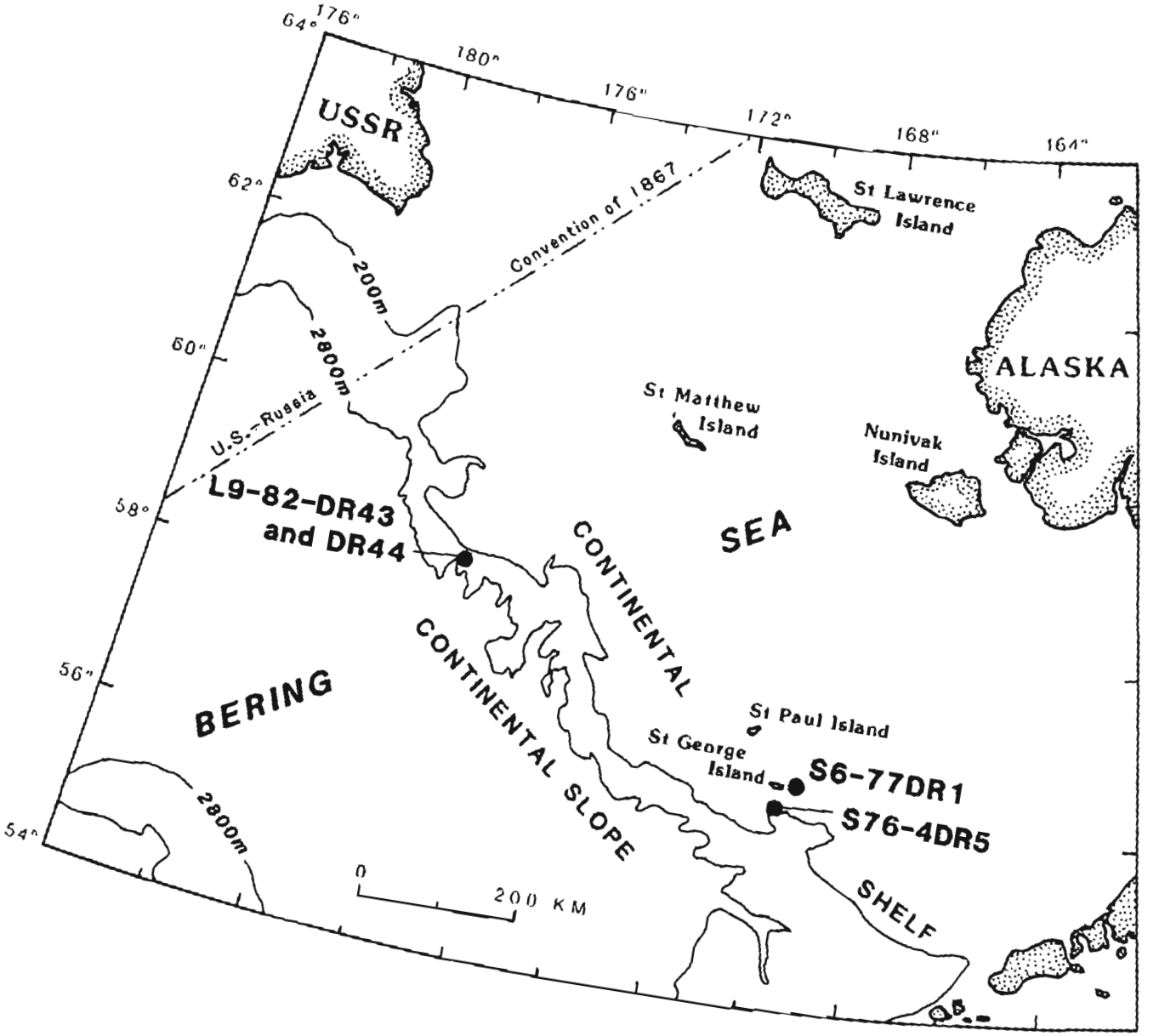
64°
176°
180°
176°
172°
168°
164°
62°
60°
58°
56°
54°
USSR
Convention of 1867
St Lawrence Island
200m
2800m
U.S.-Russia
ALASKA
St Matthew Island
Nunivak Island
L9-82-DR43 and DR44
SEA
CONTINENTAL
CONTINENTAL SLOPE
BERING
St Paul Island
St George Island
S6-77DR1
S76-4DR5
SHELF
2800m
0
200 KM

Figure 1.

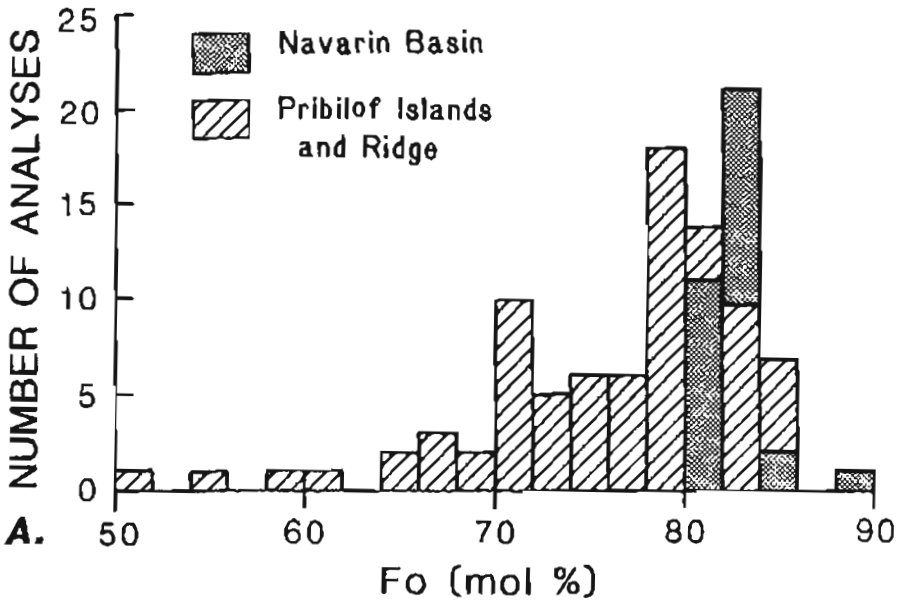
NUMBER OF ANALYSES
25
20
15
10
5
0
Navarin Basin
Pribilof Islands
and Ridge
A.
50
60
70
80
90
Fo (mol %)

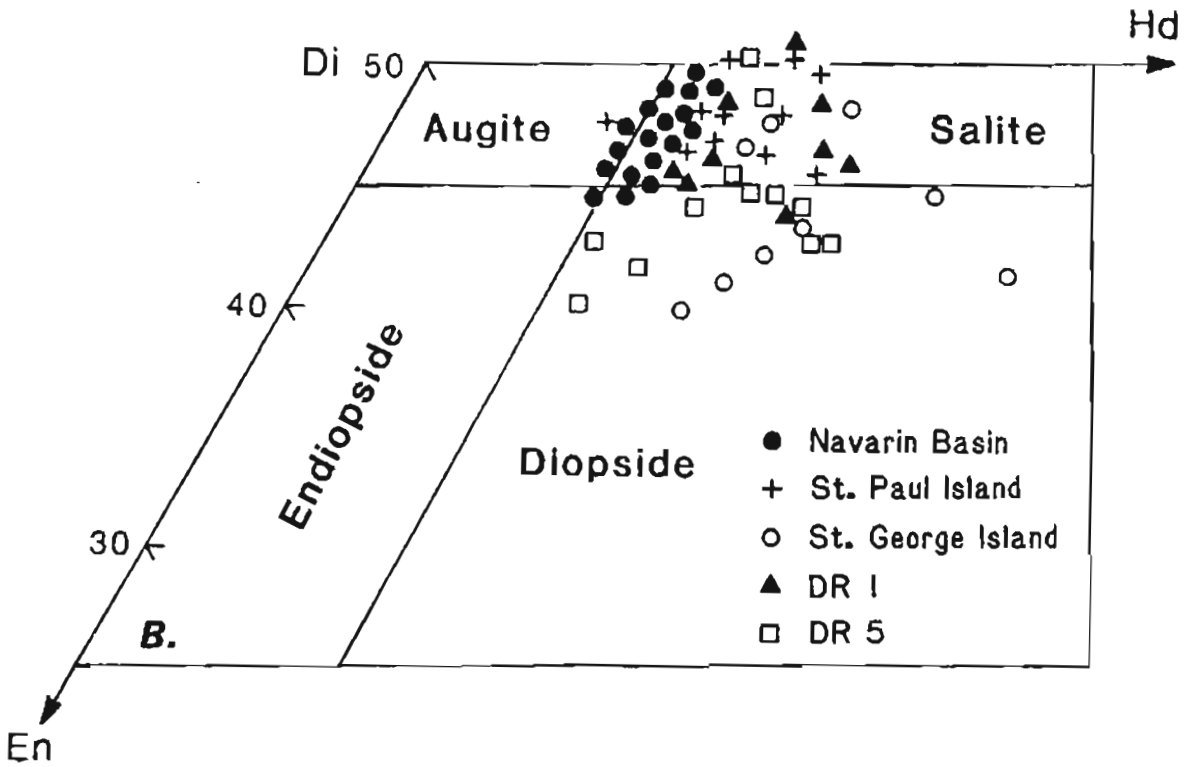
Hd
Di 50
Augite
Salite
40
Endiopside
Diopside
30
B.
En
Navarin Basin
St. Paul Island
St. George Island
DR I
DR 5

Figure 2.

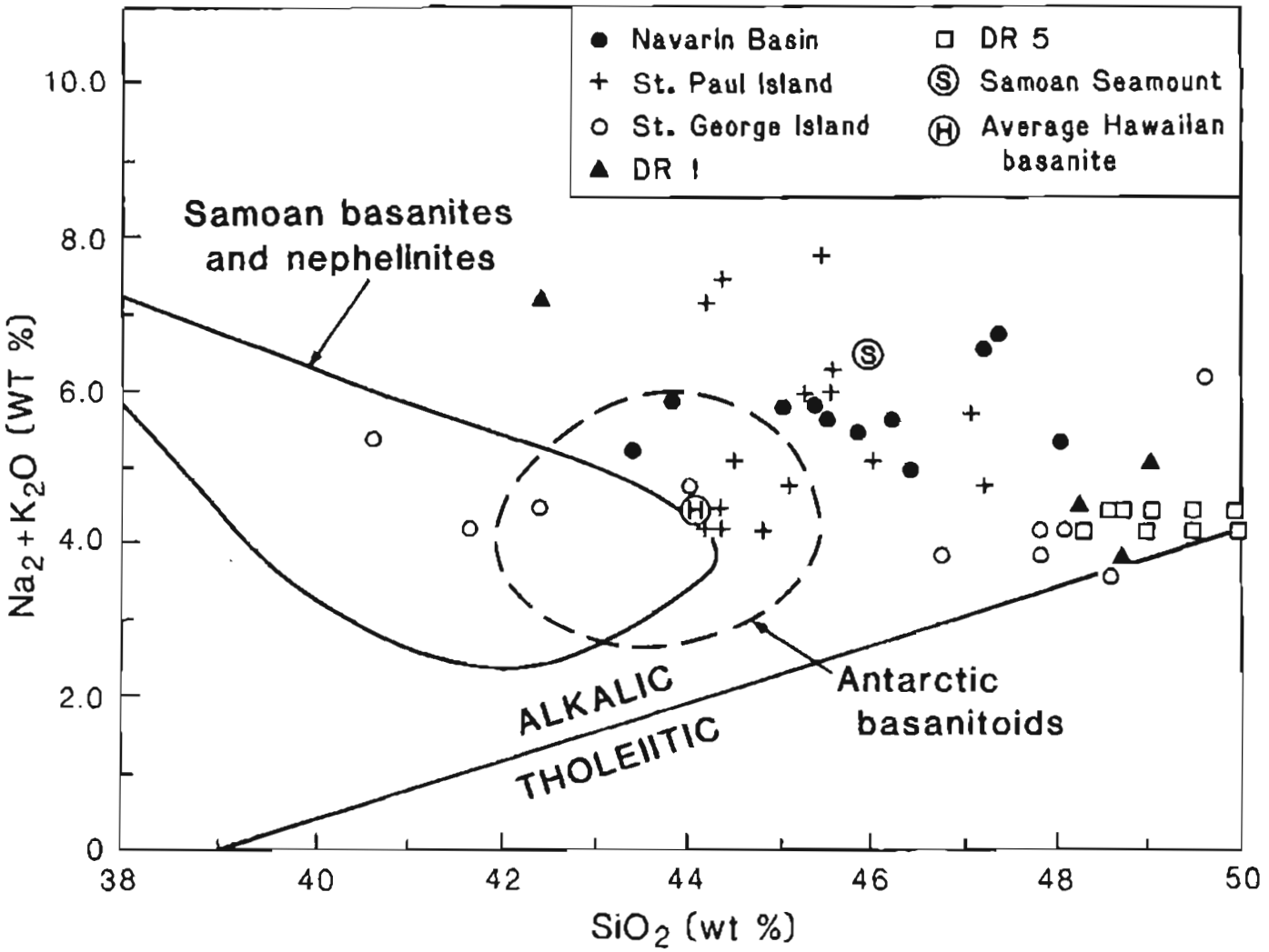
Navarin Basin
St. Paul Island
St. George Island
DR 1
DR 5
Samoan Seamount
Average Hawaiian basanite
Samoan basanites and nephelinites
ALKALIC
THOLEIITIC
Antarctic basanitoids
Na_2+K_2O (WT %)
SiO_2 (wt %)
10.0
8.0
6.0
4.0
2.0
0
38
40
42
44
46
48
50

Figure 3.

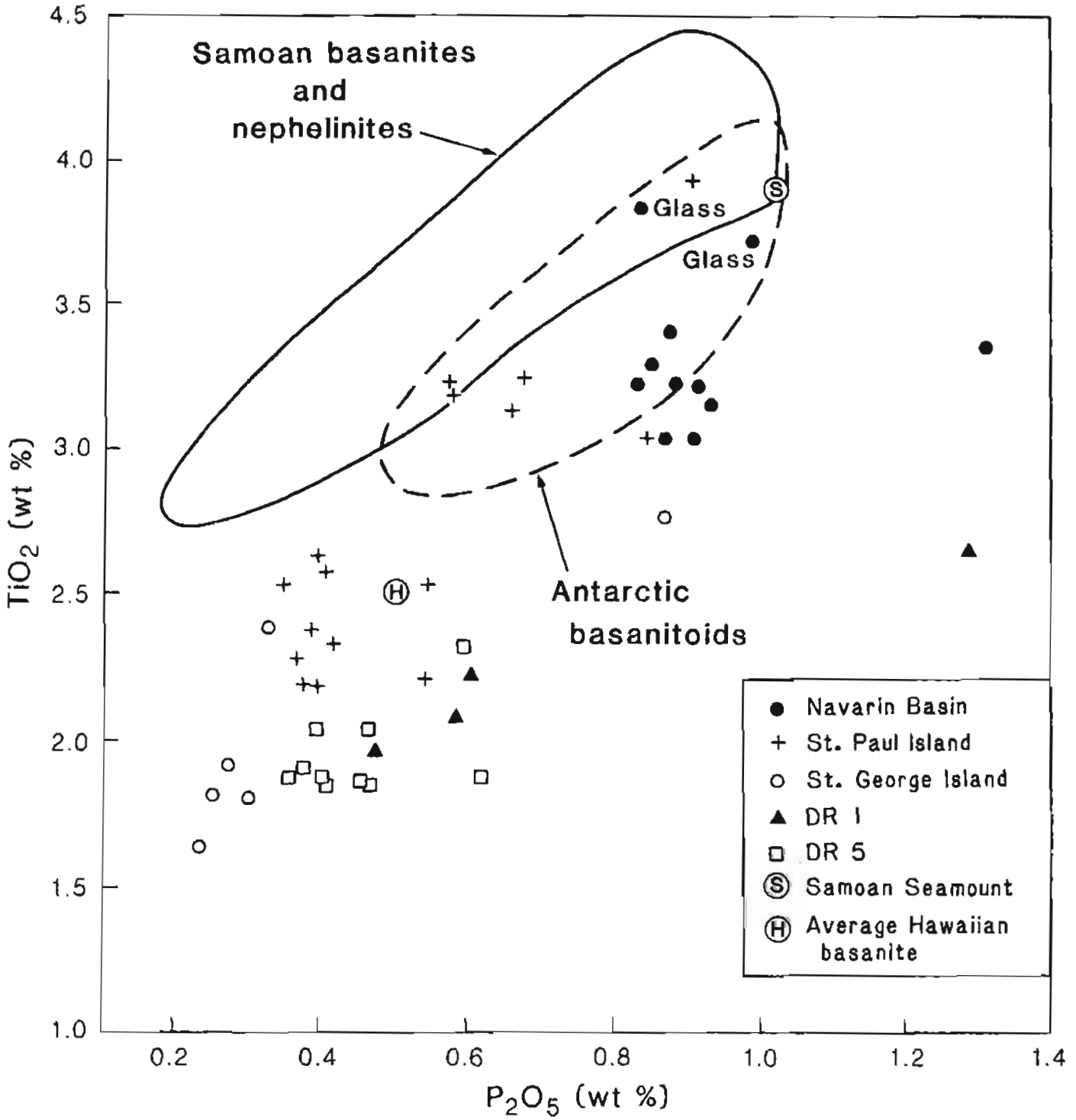
Samoan basanites and nephelinites
Glass
Glass
Antarctic basanitoids
Navarin Basin
St. Paul Island
St. George Island
DR 1
DR 5
Samoan Seamount
Average Hawaiian basanite
TiO2 (wt %)
P2O5 (wt %)
4.5
4.0
3.5
3.0
2.5
2.0
1.5
1.0
0.2
0.4
0.6
0.8
1.0
1.2
1.4

Figure 4.

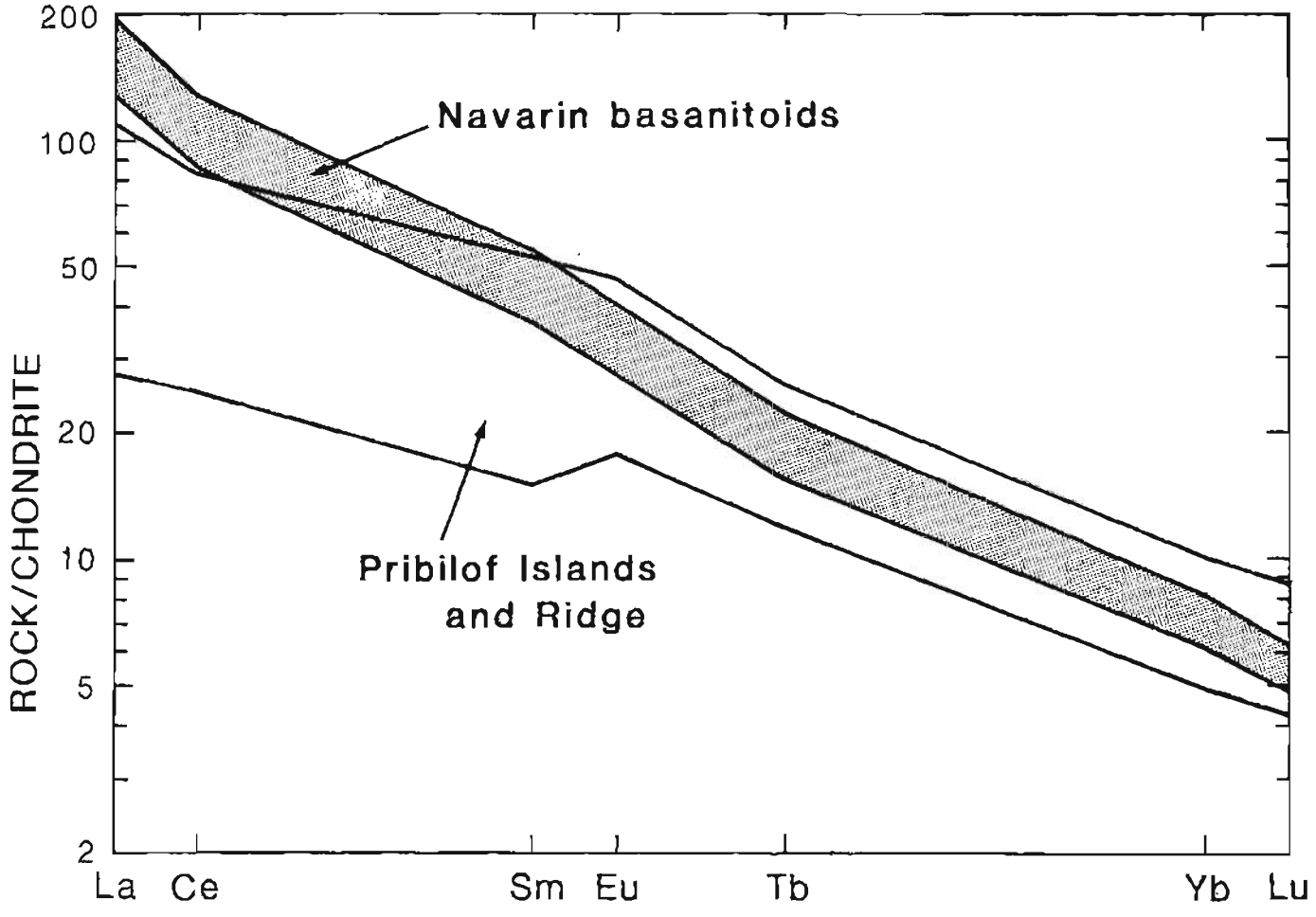
200
100
50
20
10
5
2
ROCK/CHONDRITE
Navarin basanitoids
Pribilof Islands
and Ridge
La
Ce
Sm
Eu
Tb
Yb
Lu

Figure 5.

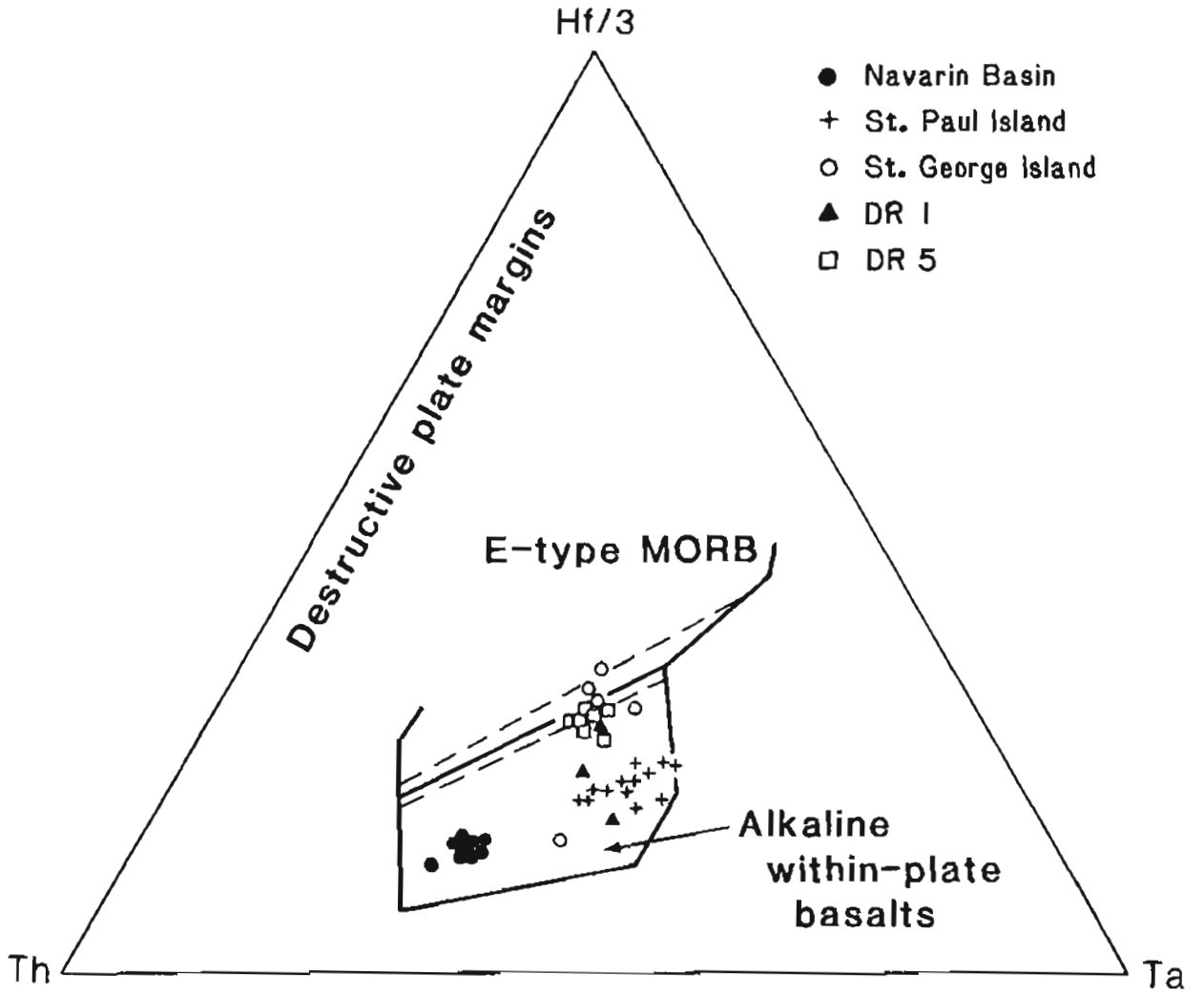
Hf/3
Th
Ta
Navarin Basin
St. Paul Island
St. George Island
DR 1
DR 5
Destructive plate margins
E-type MORB
Alkaline
within-plate
basalts

Figure 6.

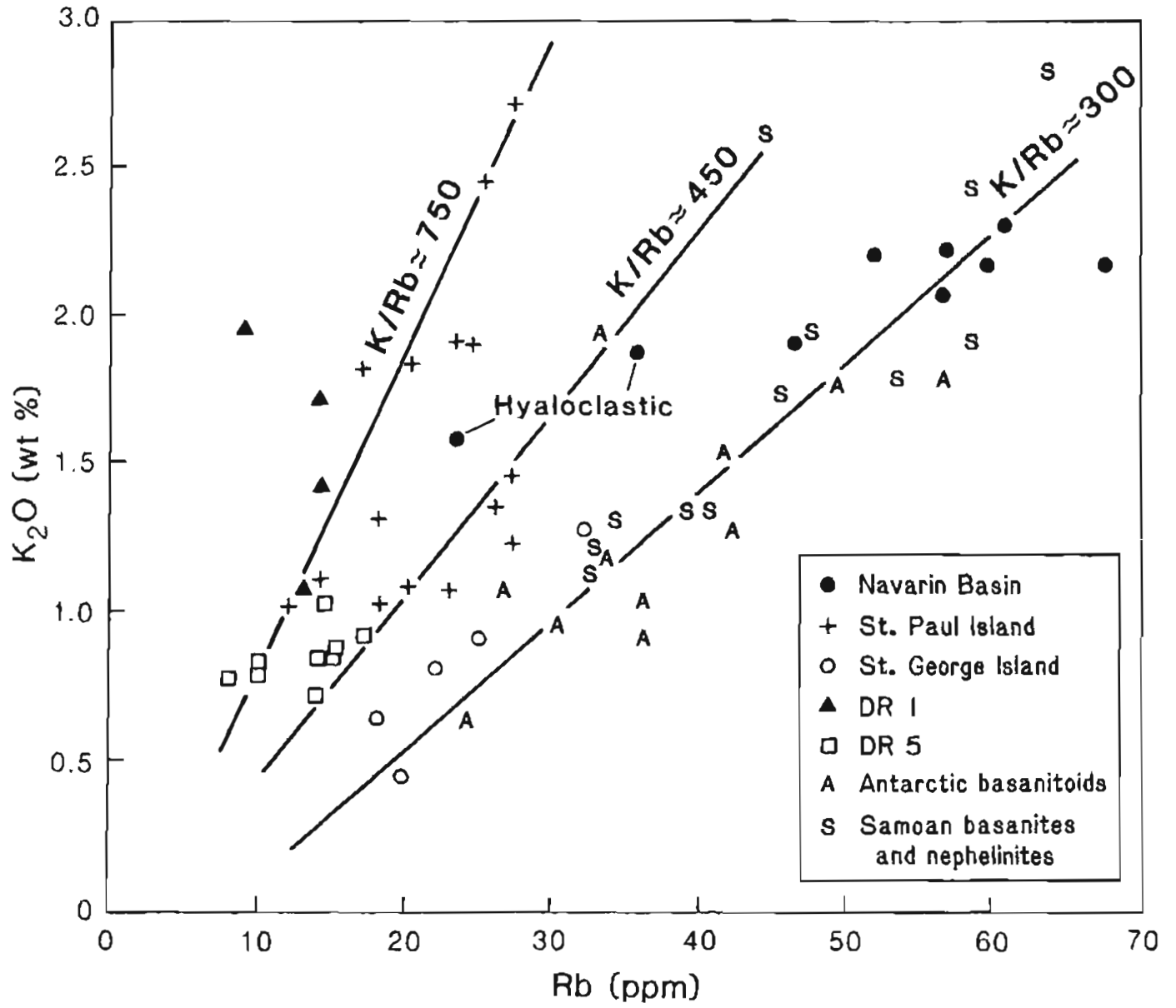
3.0
2.5
2.0
1.5
1.0
0.5
0
K_2O (wt %)
0
10
20
30
40
50
60
70
Rb (ppm)
K/Rb≈750
K/Rb≈450
K/Rb≈300
Hyaloclastic
Navarin Basin
St. Paul Island
St. George Island
DR 1
DR 5
A Antarctic basanitoids
S Samoan basanites and nephelinites

Figure 7.

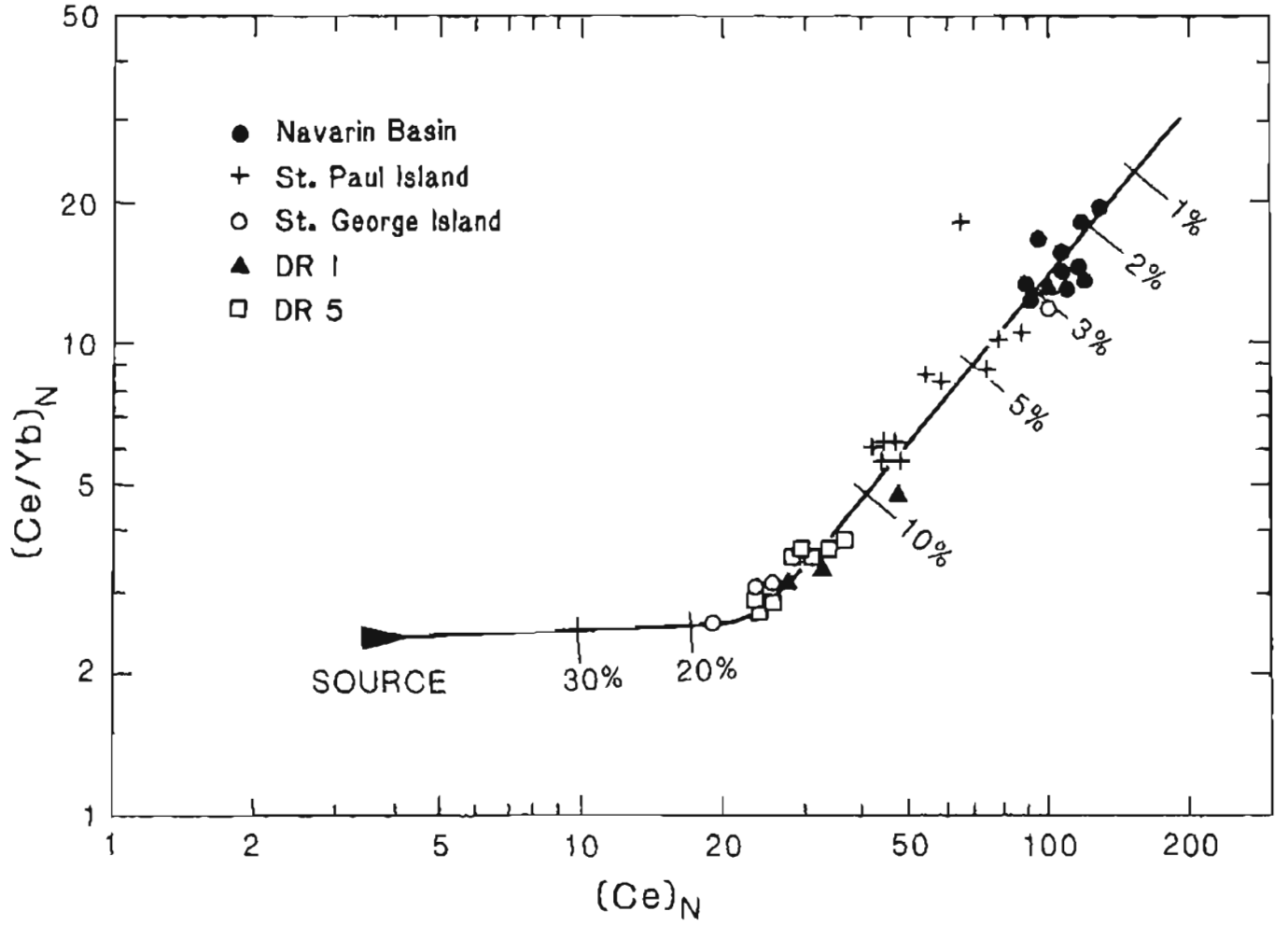
Navarin Basin
St. Paul Island
St. George Island
DR 1
DR 5
SOURCE
30%
20%
1%
2%
3%
5%
10%
(Ce/Yb)N
(Ce)N
50
20
10
5
2
1
1
2
5
10
20
50
100
200

Figure 8.

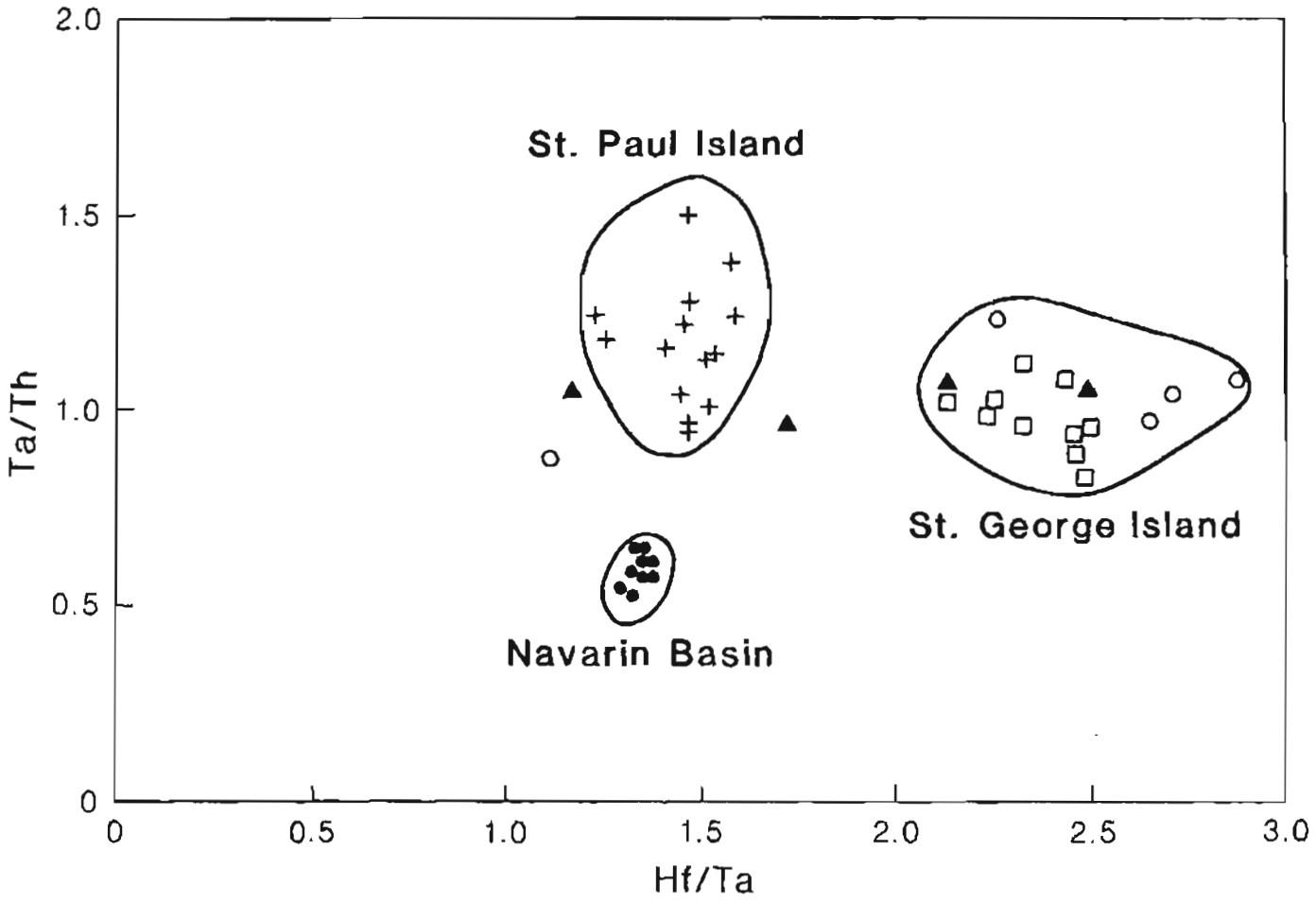
St. Paul Island
St. George Island
Navarin Basin
Ta/Th
Hf/Ta
2.0
1.5
1.0
0.5
0
0
0.5
1.0
1.5
2.0
2.5
3.0

Figure 9.